Available online at www.sciencedirect.com
SCIENCE DIRECT®
Journal of Solid State Chemistry 177 (2004) 2242–2248
JOURNAL OF SOLID STATE CHEMISTRY
http://elsevier.com/locate/jssc

Identification of charge transfer (CT) transition in (Gd,Y)BO_3:Eu phosphor under 100–300 nm

Yuhua Wang,[a,*] Xuan Guo,[a] Tadashi Endo,[b] Yukio Murakami,[c] and Mizumoto Ushirozawa[c]

[a] *Department of Materials Science, School of Physical Science and Technology, Lanzhou University, 298, Tian Shui Road, Lanzhou City 730000, PR China*

[b] *Department of Materials Chemistry, Graduate School of Engineering, Tohoku University, Sendai 980-8579, Japan*

[c] *NHK Science and Technical Research Laboratories, 1-10-11, Kinuta, Setagaya-Ku, Tokyo 157-8510, Japan*

Received 27 November 2003; received in revised form 1 March 2004; accepted 3 March 2004

Abstract

A broad excitation band in an excitation spectrum of (Gd,Y)BO_3:Eu was observed in the VUV region. It could be considered that this band was composed of two bands at about 160 and 166 nm. The preceding band was assigned to the BO_3 group absorption. The later one at about 166 nm could be assigned to the charge transfer (CT) transition of Gd^{3+}–O^{2-}. Such an assignment was deduced from the result that broadbands at around 170 nm for $GdAlO_3$:Eu, and at 183 nm for Gd_2SiO_5:Eu are due to the CT transition of Gd^{3+}–O^{2-}; this was also identified by CaZr $(BO_3)_2$:Eu. Since there are no Gd^{3+} ions in it; a weak band in the VUV region in the excitation spectrum of $Ca_{0.95}ZrEu_{0.05}(BO_3)_2$ was observed. The excitation spectra were overlapped between the CT transition of Gd^{3+}–O^{2-} and BO_3 group absorption, and it caused the emission of Eu^{3+} effectively in the trivalent europium-doped (Gd,Y)BO_3 host lattice under 147 nm excitation. Intense broad excitation bands were observed at about 155 nm for YBO_3:Eu and at about 153 nm for $YAlO_3$:Eu; it could be attributed to the CT transition between Y^{3+} and O^{2-}. As a result, under the xenon discharge (147 nm) excitation, the intense emission of Eu^{3+} in $GdBO_3$ was found to be more convenient just because of the partial substitution of Y^{3+} for Gd^{3+}.

Keywords: Yttrium gadolinium orthoborate phosphor; CT transition; Energy transition

1. Introduction

Much attention has been paid to vacuum ultraviolet (VUV) phosphors due to the demands of plasma display panels and a possible new generation of Hg-free fluorescent lamps. A fine phosphor requires strong VUV absorption, high conversion efficiency, wide color gamut and good thermal and chemical stabilities. *Ln*BO_3 (*Ln* = lanthanide, yttrium) represents a promising class of materials. Among them, (Gd,Y)BO_3 is one of the best candidates for the desired host materials of VUV phosphors, and (Gd,Y)BO_3:Eu as a red phosphor is used extensively today. However, the current phosphor is far from satisfying, because of color and efficiency problems. Moreover, the relaxation mechanism of (Gd,Y)BO_3:Eu in the VUV excitation energy region is not clear as that in the UV region. Wang et al. reported the photoluminescence of $GdAl_3(BO_3)_4$:Eu under UV and VUV regions [1]. They assigned the bands at 160 nm for (Gd,Y)BO_3:Eu and 150 nm for $GdAl_3(BO_3)_4$:Eu to the BO_3 groups absorption. Mayolet et al. [2] found that the introduction of Gd^{3+} in (Gd,La)$(BO_2)_3$, which was activated by Eu^{3+} or Tb^{3+}, increased the visible luminescence intensity considerably under the excitation of VUV (158 nm). It could be deduced from these results that BO_3 groups absorbed excitation energy transferred to the Eu^{3+} via Gd^{3+}, because the relative excitation intensities of $GdAl_3(BO_3)_4$: Eu increased with a decrease in the Eu^{3+} content under an excitation in the 150–166 nm region. But until now, the role of Gd^{3+}, Y^{3+} in borate phosphors, such as in (Gd,Y)BO_3:Eu, is not well understood. In order to understand the role of Gd^{3+} and Y^{3+}, and to identify new VUV phosphors, three types of phosphors,

*Corresponding author. Fax: +86-931-891-3554.
E-mail address: wyh@lzu.edu.cn (Y. Wang).

0022-4596/$ - see front matter © 2004 Elsevier Inc. All rights reserved.
doi:10.1016/j.jssc.2004.03.003

LnAlO_3:Eu (*Ln* = Gd,Y), Gd_2SiO_5:Eu and $CaZr(BO_3)_2$:*Eu*, were studied.

LnAlO_3:Eu(*Ln* = Gd,Y) and Gd_2SiO_5 are two important optical materials. Their luminescent properties have been discussed in the UV region (200–300 nm) [3,4]. The host lattice absorptions were reported at 8 eV (155 nm) for $YAlO_3$ [5,6] and at 6.9 eV (180 nm) for Y_2SiO_5 [7]. Such a difference arose from a different structure. *Ln*AlO_3:Eu (*Ln* = Gd,Y) is isomorphous with $GdFeO_3$ [8], crystallizing in a slightly distorted perovskite structure(*S.C.Pbnm*), with an orthorhombic unit cell. Gd^{3+} ions, which are substituted by Eu^{3+} ions, occupy the corner positions.

Both Y_2SiO_5 and Gd_2SiO_5 have a similar monoclinic lattice, but the space group is different: $P2_1/c$ for Gd_2SiO_5 [9], and $PI2/c$ for Y_2SiO_5 [10]. For Gd_2SiO_5, the Gd^{3+} ions are situated in the alternating layers; in one of these layers, the Gd^{3+} ions have a 9-fold coordination with eight oxygen atoms adjacent to the Si tetrahedral and one "free" oxygen, and in other layers, the Gd^{3+} ions have a 7-fold coordination. The coordination polyhedron is formed from four oxygen atoms of the tetrahedral and three "free" oxygens.

The compound $CaZr(BO_3)_2$ does not include the Gd^{3+} ions, which is isomorphous with dolomite, $CaMg(CO_3)_2$ [11,12]. This indicates that the crystal structure of $CaZr(BO_3)_2$ is similar to that of (Gd,Y)BO_3, which has vaterite-type structure [13]. $CaZr(BO_3)_2$ crystallizes to a dolomite structure (*S.G.R*3) with a hexagonal unit cell. The Ca^{2+} ions, which will be substituted by Eu^{3+} ions, occupy the center position.

In this paper, three types of phosphors, *Ln*AlO_3:Eu (*Ln* = Gd,Y), Gd_2SiO_5:Eu and $CaZr(BO_3)_2$:Eu, were investigated in the 100–300 nm region in order to clarify the role of Gd^{3+} (or Y^{3+}) in the energy transition process of (Gd,Y)BO_3:Eu; it is helpful to discover new VUV phosphors or improve the current phosphors.

2. Experimental

The starting materials for the preparation of *Ln*AlO_3:Eu (*Ln* = Gd,Y), Gd_2SiO_5:Eu and $CaZr(BO_3)_2$:Eu were Gd_2O_3(99.99%), Eu_2O_3 (99.99%), Y_2O_3(99.99%), $Al(NO_3)_3 \cdot 9H_2O$(98%), SiO_2(99.9%,), $CaCO_3$(99.9%,), $ZrO(NO_3)_2 \cdot 2H_2O$(97.0%) and B_2O_3(99.999%). Eu_2O_3 was heated in air at 1000°C for 24 h to remove the moisture and CO_2 present in it and then was placed in a desiccator.

The *Ln*AlO_3:Eu (*Ln* = Gd,Y) samples were prepared by the following process: the starting materials were dissolved in concentrated nitric acid, and the solution obtained was evaporated to dryness. The resulting powders were ground, pelleted and then calcined in a platinum crucible for 10 h in air at 1500°C. Polycrystalline samples doped with 5% moles of Eu^{3+} ions were obtained after cooling to room temperature under the same conditions.

Gd_2SiO_5:Eu was prepared by conventional solid state reactions. Stoichiometric proportion of the starting materials was intimately mixed together, pelleted, and then heated at 1500°C in platinum crucible in air for 24 h. Single phase activated with 5% Eu^{3+} ions was formed by cooling to room temperature in the same conditions.

The samples of $CaZr(BO_3)_2$:Eu were prepared by heating a mixture of $CaCO_3$, $ZrO(NO_3)_2 \cdot 2H_2O$ and B_2O_3 in a ratio of 1:1:2.2. The mixture was ground, pelleted and then calcined in a platinum crucible for 24 h in air at 1100°C. Polycrystalline sample doped with 5% moles of Eu^{3+} ions were fabricated in the same conditions.

The structures of these samples were identified by using an X-ray diffractometer (XRD) with Ni-filtered Cu$K\alpha$ radiation. The unit cell parameters were calculated by least-square methods with silicon powder as the internal standard. Excitation and emission spectra were measured by a Hitachi F-4500 fluorescence spectrophotometer in the UV region. Excitation spectra below 200 nm for the phosphors were recorded on an ARC Model VM-502-type vacuum monochromator. The details for the measurement conditions were described elsewhere [1]. All the spectra were recorded at room temperature.

3. Results and discussion

3.1. Identification of CT transition between Gd^{3+} and O^{2-}

3.1.1. The CT transition of Gd^{3+}–O^{2-} in several systems

Charge transfer (CT) transitions occur when a valence electron is transferred from the ligand toward the unoccupied orbitals of the metallic cation. They are partly allowed and cause, generally in the UV and VUV energy domain, very broad absorption bands that are mainly vibronic in character [14]. Since Jørgensen has assigned the broad and strong absorption band in the spectra of the trivalent lanthanides to a CT transition [15], many publications have applied such assignments in the solutions and solids [16–18].

The CT band energy appears to depend strongly on the electronegativity of ligands, the electron affinity of the metal ions and the ligand–metal distance [14]. Table 1 shows the positions of the CT transition between Gd^{3+} and O^{2-} in polycrystal systems of YF_3:(O^{2-}–Ln^{3+}), LaF_3:(O^{2-}–Ln^{3+}) and *Ln*Cl_3:(O^{2-}–Ln^{3+}); they were calculated by Jørgensen's refined spin pairing energy theory. It could generally be deduced that the CT transition energy of oxide matrices will be lower than that of fluoride and chloride matrices.

3.1.2. Identified by $Gd_{0.95}Eu_{0.05}AlO_3$

Fig. 1 shows the XRD pattern for $Gd_{0.95}Eu_{0.05}AlO_3$. $Gd_{0.95}Eu_{0.05}AlO_3$ was obtained as a single phase. This sample was indexed to an orthorhombic symmetry with the lattice parameters $a = 5.2494(2)$ Å, $b = 5.2966(2)$ Å, and $c = 7.4408(2)$ Å.

Fig. 2 shows the excitation spectrum of $Gd_{0.95}Eu_{0.05}AlO_3$. The spectrum was composed of two bands with maxima at about 170 and 265 nm. As shown in Ref. [3], the broad 265 nm band was identified as the CT transition between Eu^{3+} and O^{2-}; this was an electron transfer from $O^{2-}(2p^6)$ orbital to the empty orbital of 4f for Eu^{3+}. The 170 nm band in the excitation spectrum of $Gd_{0.95}Eu_{0.05}AlO_3$ could be assigned to the CT transition between Gd^{3+} and O^{2-}.

Under 147 excitation, $Gd_{0.95}Eu_{0.05}AlO_3$ exhibits a bright red luminescence (613 nm) with CIE chromaticity coordinates of (0.623, 0.335) with a PL intensity of 70 of the commercial phosphor $(Gd,Y)BO_3:Eu^{3+}$ (KX-504A).

3.1.3. Identified by $Gd_{1.95}Eu_{0.05}SiO_5$

As shown in Fig. 3, $Gd_{1.95}Eu_{0.05}SiO_5$ was indexed to a monoclinic symmetry with lattice parameters $a = 9.1323(2)$ Å, $b = 7.0574(2)$ Å, and $c = 6.7510(2)$ Å, $\beta = 107.51°$. XRD patterns of Gd_2SiO_5 doped and undoped with Eu^{3+} showed the formation of a single phase.

Table 1
The positions of the CT transition of Gd^{3+}–O^2

System	Position of CT transition (λ_{max}, nm)	Ref.
YF_3	≈123	[19]
LaF_3	≈131	[19]
$LnCl_3$	≈135	[15]

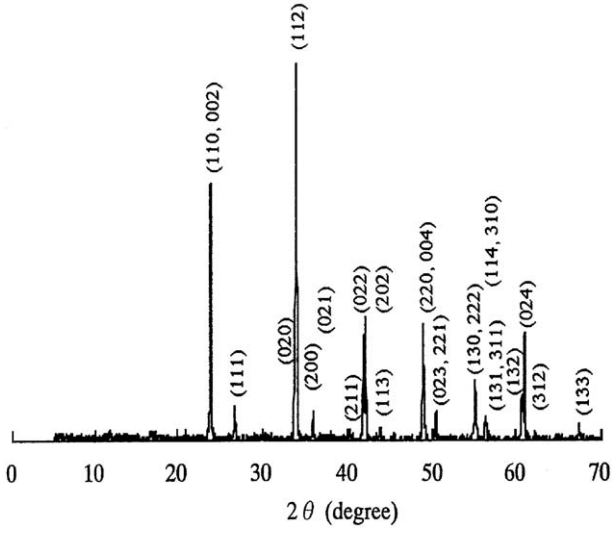

Fig. 1. XRD pattern of $Gd_{0.95}Eu_{0.05}AlO_3$.

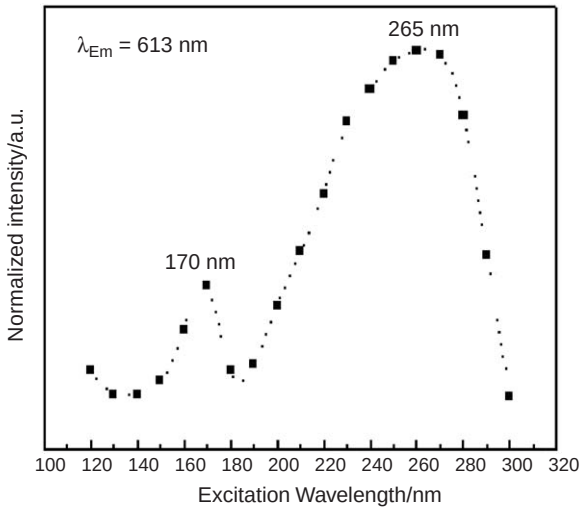

Fig. 2. Excitation spectrum of $Gd_{0.95}Eu_{0.05}AlO_3$.

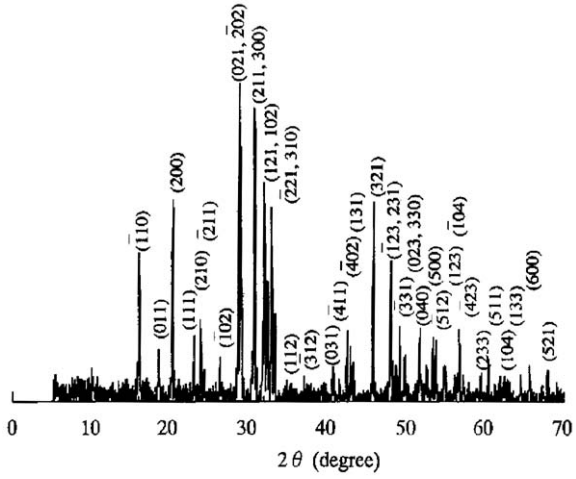

Fig. 3. XRD pattern of $Gd_{1.95}Eu_{0.05}SiO_5$.

Fig. 4 shows the excitation spectrum of $Gd_{1.95}Eu_{0.05}SiO_5$. Two bands were observed at around 183 and 253 nm: the 253 nm band was assigned to CT transition of Eu^{3+}–O^{2-} [20], and the 183 nm band was assigned to the CT transition between Gd^{3+} and O^{2-}.

Under 147 excitation, $Gd_{1.95}Eu_{0.05}SiO_5$ exhibits a bright red luminescence (613 nm) with a PL intensity of 20 of the commercial phosphor $(Gd,Y)BO_3:Eu^{3+}$ (KX-504A). This phosphor is not effectively under 147 nm excitation. This is due to the unfavorable excitation spectral position, which was determined by the free O^{2-}.

Table 2 shows the positions of the CT transition between Gd^{3+} and O^{2-} in several oxide phosphors. These data indicated that bands observed in the 160–183 nm region could be associated with the CT transition between Gd^{3+} and O^{2-}. The CT transition between Gd^{3+} and O^{2-} is realized at different energy levels, corresponding to the different crystal structures. For

instance, the CT transitions of Gd_2SiO_5:Eu and $Ca_4GdO(BO_3)_3$:Eu were positioned at the lower-energy sides than (Gd,Y)BO_3:Eu; this is due to the different surroundings of the activator, and some free oxygens, which readily give their own electrons for transferring, participated in the crystal structures of Gd_2SiO_5:Eu and $Ca_4GdO(BO_3)_3$:Eu. This will be discussed elsewhere in detail.

3.1.4. Identified by $Ca_{0.95}ZrEu_{0.05}(BO_3)_2$

Fig. 5 shows the diffraction pattern of $Ca_{0.95}ZrEu_{0.05}(BO_3)_2$; it was indexed as hexagonal symmetry with the lattice parameters $a = 4.9328(2)$ Å, and $c = 16.1337(2)$ Å.

In Fig. 6, the CT transition between Eu^{3+} and O^{2-} was observed in the excitation spectrum of $Ca_{0.95}ZrEu_{0.05}(BO_3)_2$ at around 260 nm, but in a VUV region (<200 nm), the excitation band is weak, which may be due to BO_3 absorption. The result indicates that Gd^{3+} plays a significant role in the optical absorption of excitation energy.

3.1.5. Identification of CT transition of Gd^{3+}–O^{2-} in (Gd, Y)BO_3:Eu

Fig. 7 shows the excitation spectrum of commercially available (Gd,Y)BO_3:Eu separately. The excitation spectrum closely resembles that reported by Koike and Kojima [21]. Two bands banding at 166 and 227 nm were observed. The 227 nm band is assigned to the CT transition between Eu^{3+} and O^{2-} [15]. As judged from the vacuum excitation spectra of $Gd_{0.95}Eu_{0.05}AlO_3$, $Gd_{1.95}Eu_{0.05}SiO_5$ and $Ca_{0.95}ZrEu_{0.05}(BO_3)_2$, the broad-band at about 166 nm could be assigned to CT transition between Gd^{3+} and O^{2-} in the excitation spectrum of (Gd,Y)BO_3:Eu. From the discussion above, it is clear that the bands which were observed for (Gd,Y)BO_3:Eu in the VUV region can be assigned to BO_3 absorption (160 nm) and CT transition between Gd^{3+} and O^{2-} (166 nm), respectively. The excitation energy transfer from BO_3 groups to Eu^{3+} ions via Gd^{3+} ions could be explained in terms of excitation spectra overlap between the CT transition of Gd^{3+}–O^{2-} and BO_3 group absorption.

In (Gd,Y)BO_3:Eu, the excitation energy transfer from BO_3 group absorption to rare earths was probably realized by exchange processes as argued by Dexter [22]. The probability of energy transfer required both the wave function overlap and the energy overlap. Such requirement was well satisfied in yttrium gadolinium orthoborate phosphor, because the excitation energy was overlapped between the CT transition of Gd^{3+}–O^{2-} and the optical absorption of BO_3 groups. As a consequence, it was found that the energy transfer from BO_3 groups to Gd^{3+} ions was very efficient in (Gd,Y)BO_3 with vaterite-type structure [13]. In vaterite-type structure, the rare earths were surrounded by

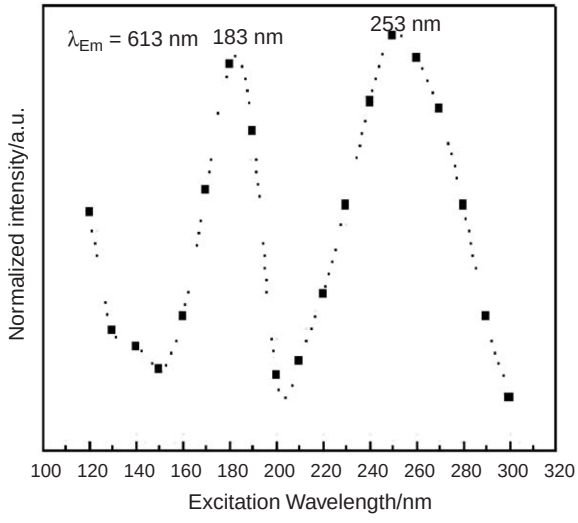

Fig. 4. Excitation spectrum of $Gd_{1.95}Eu_{0.05}SiO_5$.

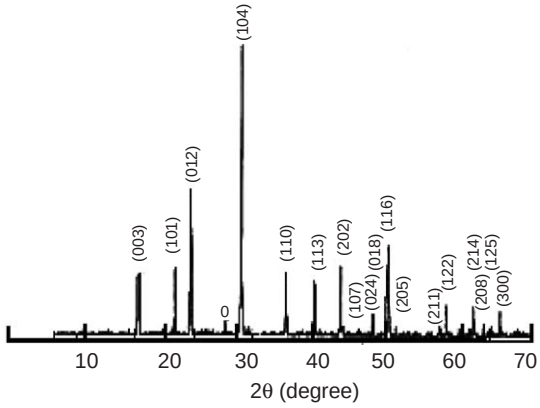

Fig. 5. XRD pattern of $Ca_{0.95}ZrEu_{0.05}(BO_3)_2$.

Table 2
Properties of some Eu^{3+}-activated oxides

Phosphor	Crystal	Position of CT (λ_{max}, nm)	Ref.
$GdBO_3:Eu^{3+}$	Vaterite	166	[1]
(Gd,Y)$BO_3:Eu^{3+}$ (KX-504A)	Vaterite	166	[1]
$GdAl_3(BO_3)_4:Eu^{3+}$	Huntite	160	[1]
$GdAlO_3$:Eu3+	Perovskite	170	This work
$Gd_2SiO_5:Eu^{3+}$	Oxyorthosilicate	183	This work
$Ca_4GdO(BO_3)_3:Eu^{3+}$	Fluorapatite	184	This work

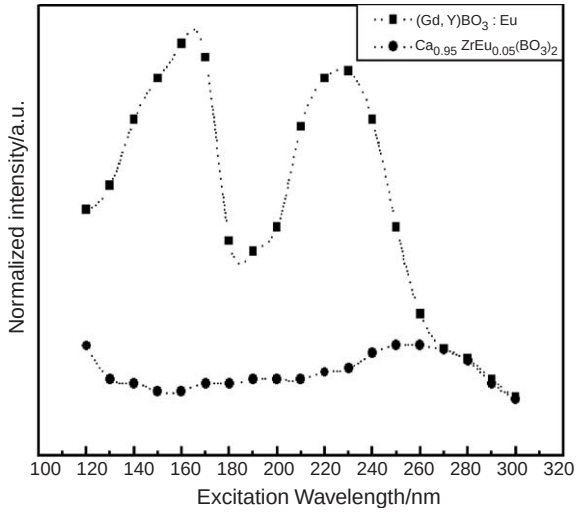

Fig. 6. Excitation spectra of $Ca_{0.95}ZrEu_{0.05}(BO_3)_2$ and $(Gd,Y)BO_3$:Eu(KX-504A). ($\lambda_{Em} = 613$ nm).

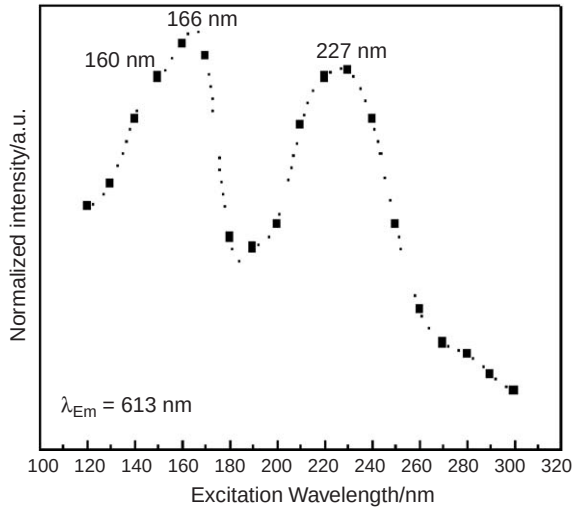

Fig. 7. Excitation spectrum of $(Gd,Y)BO_3$:Eu (KX-504A).

the BO_3 groups and possessed a center of symmetry. The requirement of energy overlap (of the emission of Gd^{3+} ions and the absorption of the Eu^{3+} ions) was satisfactory, because the excited Gd^{3+} states were situated at a position higher than the $^5D_0$ state of the Eu^{3+} so that the energy transfer from Gd^{3+} to Eu^{3+} was possible [23]. This elucidation was supported by the fact that $(Gd,Y)BO_3$:Eu was efficient as red phosphor under VUV excitation (147 nm).

3.2. Identification of CT transition between Y^{3+} and O^2

$Y_{0.95}Eu_{0.05}AlO_3$ was indexed to an orthorhombic structure with the lattice parameters $a = 5.3208(2)$ Å, $b = 7.3702(2)$ Å, and $c = 5.1791(2)$ Å as shown in Fig. 8, and traces of $Y_3Al_5O_{12}$ were observed as a second phase in $YAlO_3$:Eu.

Occasionally, the structural stability of perovskite-type $LnAlO_3$ was predicted by using the tolerance factors. On passing through the series of rare-earth elements from La to Yb, the structural stability of $LnAlO_3$ had, in fact, gradually decreased [24]. As far as the size of ionic radii of rare earth is concerned, the decomposition of $YAlO_3$ was possible under the present synthetic conditions.

Fig. 9 shows the excitation spectrum of $Y_{0.95}Eu_{0.05}AlO_3$. The excitation spectrum contained two bands at about 250 and 153 nm. The 250 nm band was assigned to the CT transition between Eu^{3+} and O^{2-} as shown in the literature [3]. On the other hand, the 153 nm band was related to the CT transition between Y^{3+} and O^{2-}. Such assignment had been done on the basis of which the intense absorption band was observed near 155 nm in $YAlO_3$ doped with trivalent rare-earth ions (Ce^{3+}, Tb^{3+}, etc.), and this band was assigned to the electronic transitions of O^{2-}:$2P^6$ to Y^{3+}:$4P^6$ ($4d + 5s$) [5–7,9]. As mentioned before, the CT band energy appears to depend strongly on the ligand–metal distance. The bond length of Y^{3+}–O^{2-} and the corresponding position of excitation band were listed in Table 3. In isostructural host lattices, CT absorption bands shift to a longer wavelength when the rare-earth ion is incorporated on a larger cationic site. On the other hand, in different crystal structures, we can use the bond length on average to evaluate the CT properties. This is due to the fact that when the bond length on average increased the ionicity of the metal–ligand, bonding increased, so the CTs shift to the shorter energy as shown in Table 3.

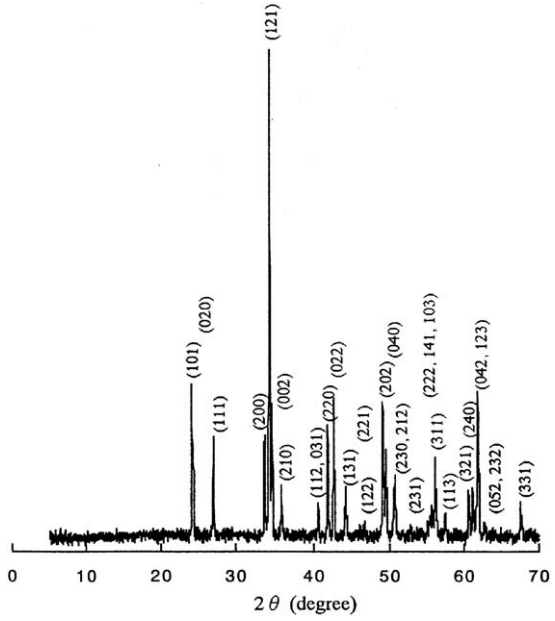

Fig. 8. XRD pattern of $Y_{0.95}Eu_{0.05}AlO_3$.

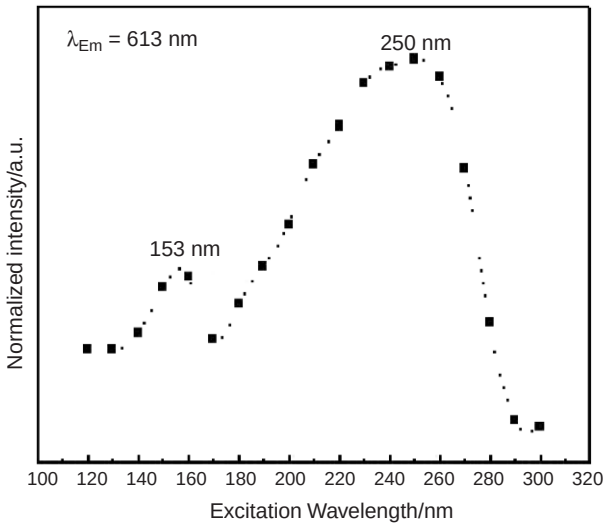

Fig. 9. Excitation spectrum of $Y_{0.95}Eu_{0.05}AlO_3$.

Table 3
The bond length of Y^{3+}–O^{2-} and the corresponding position of excitation band

Phosphor	Bondlength (Å)	Average (Å)	Position of CT (λ_{max}, nm)	Ref.
Y_2O_3:Eu^{3+}	2.284 2.248 2.279 2.336	2.287	203	[25]
YBO_3:Eu^{3+}	2.386 × 6 2.323 × 2	2.370	164	This work
$YAlO_3$:Eu^{3+}	2.797 2.213 3.164 2.471 3.259 2.339 2.656 2.338	2.657	153	This work

It was seen that the excitation band was associated with the bond length (in average) of Y^{3+}–O^{2-}. Consequently, the 153 nm band of $YAlO_3$:Eu can be assigned to the CT transition from O^{2-}:$2P^6$ to Y^{3+}:$4P^6(4d+5s)$. This indicated that the CT transition between Y^{3+} and O^{2-} played a significant role in the optical absorption of excitation energy.

The PL spectrum of $Y_{0.95}Eu_{0.05}AlO_3$ is similar to that of $Gd_{0.95}Eu_{0.05}AlO_3$. Calculation of the color coordinates gives $x = 0.636$, $y = 0.340$ with a PL intensity of 60 of the (Gd,Y)BO_3:Eu^{3+} (KX-504A) for $Y_{0.95}Eu_{0.05}AlO_3$, and confirms that it has the appearance of pure spectral red, corresponding approximately to 613 nm.

Accordingly, the excitation and emission processes of (Gd,Y)BO_3:Eu phosphor were schematically illustrated in Fig. 10. This scheme is plausible because we did

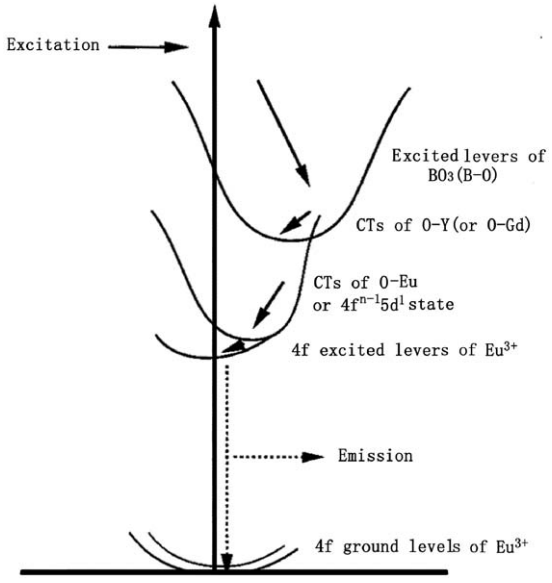

Fig. 10. Emission processes of Eu^{3+} ion in (Gd,Y)BO_3:Eu.

observe the efficient emission of (Gd,Y)BO_3:Eu under the 147 nm VUV excitation by Xe discharge.

4. Conclusions

(1) In the excitation spectrum of (Gd,Y)BO_3:Eu, two bands were observed at about 160 and 166 nm, the latter one corresponding to the CT transition between Gd^{3+} and O^{2-}. Such identification was given by the analogism that the CT transition between Gd^{3+} and O^{2-} at 170 nm for $GdAlO_3$ and 183 nm for Gd_2SiO_5, and for $Ca_{0.95}ZrEu_{0.05}(BO_3)_2$, only a weak excitation band was observed. Accordingly, the energy transfer from host lattice to Eu^{3+} ions was understood in terms of excitation spectra overlapped between CT transition of Gd^{3+}–O^{2-} and BO_3 group absorption.

(2) Under 147 nm excitation, it was observed that the emission of YBO_3:Eu took place efficiently, owing to the CT transition between Y^{3+} and O^{2-}. This identification was in agreement with our observation in $YAlO_3$:Eu, which was excited effectively at 153 nm due to the CT transition between Y^{3+} and O^{2-}.

In this context, it was clear that the emission of Eu^{3+} was induced by the wave functions overlapping between the CT transition of Gd^{3+}–O^{2-} (or Y^{3+}–O^{2-}) and BO_3 group absorption in (Gd,Y)BO_3:Eu.

Acknowledgments

This project is supported by the Ministry of Science and Technology of China, and by a Grant-in-Aid for Scientific Research (B) (2) 11555232 of the Ministry of

Education, Science and Culture, Japan, the NSFC (50272026) and EYTP (Excellent Young Teachers Program of M0E, China).

References

[1] Y.H. Wang, K. Uheda, H. Takizawa, U. Mizumoto, T. Endo, J. Electeochem. Soc. 148 (2001) 6430.
[2] A. Mayolet, W. Zhang, P. Martin, B. Chassigneux, J.C. Krupa, J. Electrochem. Soc. 143 (1996) 330.
[3] M.J. Weber, Phys. Rev. B 8 (1973) 54.
[4] J. Hölsä, K. Jyrkäs, M. Leskelä, J. Less-Common Met. 126 (1986) 215.
[5] V.N. Abramov, A.I. Kuznetsov, Sov. Phys. Solid State 20 (1978) 399.
[6] T. Tomiki, H. Ishikawa, T. Tashiro, M. Katsuren, A. Yonesu, T. Hotta, T. Yabiku, M. Akamine, T. Futemma, T. Nakaoka, I. Miyazato, J. Phys. Soc. Japan 64 (1995) 4442.
[7] A. Mayolet, J.C. Krupa, J. Soc. Int. Disp. 3 (1996) 173.
[8] S. Geller, E.A. Wood, Acta Crystallogr. 9 (1956) 563.
[9] Yu.I. Smolin, S.P. Tkachev, Kristallografiya 14 (1969) 22.
[10] B.A. Maksimov, Y.A. Kharitonov, V.V. Ilyukhin, N.V. Belov, Dokl. Akad. Nauk USSR 183 (1968) 1072;
B.A. Maksimov, Y.A. Kharitonov, V.V. Ilyukhin, N.V. Belov, Sov. Phys. Dokl. 13 (1969) 1188.
[11] V.D. Schultze, et al., Z. Anorg. Allgem. Chem. 380 (1971) 37.
[12] R.A. Howie, F.M. Broadhurst, Am. Miner. 43 (1958) 1210.
[13] E.M. Levin, R.S. Roth, J.B. Martin, Am. Miner. 46 (1961) 1030.
[14] J.C. Krupa, J. Alloys Compd. 225 (1995) 1.
[15] (a) C.K. Jørgensen, Mol. Phys. 5 (1962) 271;
(b) C.K. Jørgensen, et al., Z. Naturforschg. 20a (1965) 54.
[16] J.C. Barnes, F.M.H. Pincott, J. Chem. Soc. A (1966) 842.
[17] L.J. Nugent, R.D. Baybarz, J.L. Burnett, J.L. Ryan, J. Inorg. Nucl. Chem. 33 (1971) 2503.
[18] L.J. Nugent, R.D. Baybarz, J.L. Burnett, J.L. Ryan, J. Phys. Chem. 73 (1969) 1177.
[19] I. Gérard, J.C. Krupa, E. Simoni, P. Martin, J. Alloys Compd. 207/208 (1994) 120.
[20] G. Blasse, A. Bril, Philips Res. Rep. 22 (1966) 2356.
[21] J. Koike, T. Kojima, R. Toyonaga, J. Electrochem Soc. 126 (1979) 1008.
[22] D.L. Dexter, J. Chem. Phys. 21 (1953) 836.
[23] A. Bril, W.L. Wanmaker, J. Electrochem. Soc. 111 (1964) 1363.
[24] I. Warshaw, R. Roy, J. Am. Ceram. Soc. 42 (9) (1959) 434.
[25] C.R. Ronda, J. Lumin. 72–74 (1997) 49.